Effect of Fuel Unsaturation on Emissions in Flames and Diesel Engines

Suresh K. Aggarwal

Abstract Due to the emergence of a new generation of renewable fuels and the need to accurately model the combustion chemistry of multi-component fuels, there is growing interest in examining the effect of fuel molecular structure on fuel reactivity. This book chapter provides an overview of research dealing with the effects of fuel unsaturation on the ignition, combustion, and emission characteristics. Results from both laboratory-scale configurations, such as shock tube, rapid compression machine, and laminar flames, as well as from high-pressure sprays in compression ignition engines are discussed. Experimental and kinetic modeling studies of homogeneous mixtures provide clear evidence that depending upon the number and position of C = C double bonds, and the reactivity of long-chain hydrocarbons is significantly affected by fuel unsaturation, especially at low to intermediate temperatures. Ignition data for saturated and unsaturated components indicate that the presence of double bond inhibits low-temperature reactivity, modifies the NTC behavior, and leads to reduction in CN number in diesel engines. This has important consequences regarding the effect of unsaturation on combustion and emission in practical systems. High-pressure spray simulations under diesel engine conditions indicate longer ignition delays for 1-heptene compared to those for n-heptane. In addition, the n-heptane spray flame contains two reaction zones, namely a rich premixed zone (RPZ) and a nonpremixed reaction zone (NPZ). In contrast, 1-heptene flame is characterized by three reaction zones, i.e., a lean premixed zone (LPZ) in addition to NPZ and RPZ. Simulations of laminar partially premixed flames (PPF) indicate higher amounts of NOx and soot precursor species (C_2H_2, C_6H_6, and $C_{16}H_{10}$) formed in 1-heptene flames than those in n-heptane flames. Consequently, the soot emission is higher in 1-heptene flames than that in n-heptane flames. Simulations of turbulent n-heptane and 1-heptene spray flames in diesel engines lead to similar conclusions, i.e., higher NOx and soot emissions in 1-heptene flames. The increased formation of PAH species can be attributed to the significantly higher amounts of 1,3-butadiene and allene formed due to β scission reactions resulting from the presence of double bond in 1-heptene.

S. K. Aggarwal (✉)
University of Illinois at Chicago, Chicago, IL, USA
e-mail: ska@uic.edu

© Springer Nature Singapore Pte Ltd. 2018

A. K. Runchal et al. (eds.), *Energy for Propulsion*, Green Energy and Technology,
https://doi.org/10.1007/978-981-10-7473-8_3

Keywords Fuel unsaturation · Ignitability · Two-stage ignition · Soot precursors NOx and soot emissions

1 Introduction

There is growing interest in investigating the effect of fuel molecular structure on fuel reactivity and thus on the ignition and combustion characteristics. This has been driven by several considerations, such as the emergence of a new generation of renewable fuels, and the recognition that the combustion chemistry of real fuels cannot be modeled using single-component fuels, and that many conventional and emerging fuels contain a number of saturated and unsaturated hydrocarbon compounds. For instance, biodiesel fuels produced using the trans-esterification process contain a relatively large amount of unsaturated ester components, and the molecular structure of these components can vary significantly with respect to the number and location of C = C bonds, depending upon the feedstock. As a result, their reactivity and cetane number (CN) can vary significantly [1], with each C = C double bond in the long carbon chain of component molecule reducing the CN value by a significant amount [2]. For example, palm oil methyl ester with high fraction of saturated components, such as methyl stearate ($C_{19}H_{38}O_2$), has a CN of 62, whereas linseed oil methyl ester containing high fraction of methyl linolenate ($C_{19}H_{32}O_2$) with three C = C double bonds has a CN of 39, implying significant reduction in ignitability. Another important issue pertains the effect of fuel molecular structure on the fuel sensitivity (S), which is defined as the difference between research octane number (RON) and motor octane number (MON). Several recent studies have shown that ignitability is determined by both fuel octane rating and sensitivity [3, 4]. Sensitivity provides a measure of aromatic and other non-paraffinic content of the fuel, and high sensitivity fuels exhibit different temperature dependence at low, medium, and high temperatures. Experimental studies using homogeneous mixtures in shock tube (ST) and rapid compression machine (RCM) have reported that these fuels have low reactivity at low temperatures, but react rapidly at high temperatures, and exhibit varying degrees of negative temperature coefficient (NTC) behavior [4, 5]. Previous research has also shown that primary reference fuels (PRF), for which S = 0, are not able to emulate this temperature dependence. Moreover, sensitivity is strongly related not only to fuel composition but also to its molecular structure or level of unsaturation. For example, as reported by Tanaka et al. [6], S = 0 for n-heptane (alkane) and 13 for 1-heptene (alkene with a C = C bond). Finally, there is also fundamental interest in examining the pyrolysis/oxidation chemistry of alkenes, since such compounds are formed during the combustion of alkanes.

This chapter provides an overview of research dealing with the effects of fuel unsaturation on the ignition, combustion, and emission characteristics. A considerable research exists on this topic. Many experimental investigations have reported ignition data from ST and RCM experiments for different fuels and over a wide range of conditions. Complementary kinetic studies have also been performed to

examine the reaction pathways during the pyrolysis/oxidation of saturated and unsaturated fuels and develop reaction mechanisms for predicting the ignition behavior of these fuels under homogeneous condition. This work is briefly reviewed. In addition, research dealing with laboratory-scale laminar flames and diesel sprays using saturated and unsaturated surrogates is briefly discussed. Experimental engine studies concerning the emission characteristics of various biodiesel fuels are also mentioned. As expected, the scope of this chapter is limited due to the broad range of topics covered and also due to the page limitation. It does not include details of the experimental methods and the physical-computational models used in simulations. Most of the discussion and results are taken from previously reported work, which is appropriately cited.

2 Effect of Unsaturation on Ignition in Homogeneous Mixtures

Fundamental investigations on the ignition of homogeneous fuel–air mixtures provide valuable information for the development and validation of reaction mechanisms. Such data is also useful for understanding ignition delays and burning rates in homogeneous charge compression ignition (HCCI) engines and examining knocking behavior in spark-ignition engines. Numerical algorithms and software, such as CHEMKIN-Pro [7] and Cantera [8], are being extensively used to examine ignition characteristics, validate reaction mechanisms, and analyze reaction pathways under constant volume or constant pressure conditions. Ignition characteristics include the ignition delay time as a function of system properties, such as temperature, pressure, equivalence ratio (ϕ), fuel composition, and two-stage ignition and negative temperature coefficient (NTC) phenomena. While straight chain alkanes have been extensively investigated, some experimental and modeling studies have also examined the oxidation of straight chain C_5, C_6, and C_7 alkene isomers. Various surrogates[1] of current and emerging fuels, such as diesel, gasoline, JP-8, and biofuels, have also been analyzed. Ignition delay and speciation data have been reported from shock tube [6, 9–11], RCM [12, 13], and flow reactor [14] experiments. Detailed kinetic models have also been developed to provide insight into the effects of the presence and position of double bonds on fuel reactivity and ignitibility [15, 16].

Tanaka et al. [6] and Vanhove et al. [13] performed RCM experiments and examined the effects of fuel molecular structure on ignition. Tanaka et al. [6] reported ignition data for several saturated and unsaturated hydrocarbons and analyzed the two-stage ignition and NTC behavior. Representative results from this work are provided in Figs. 1 and 2. Figure 1 presents data on ignition delays for several hydrocarbons. An important observation is the existence of two-stage ignition and NTC phenomenon for n-heptane, 1-heptene, and 2-heptene, but only a single-stage ignition for 3-heptene. In addition, results indicate longer ignition delays for unsaturated

[1] Such surrogates are not discussed in this chapter as the main topic is the effect of fuel unsaturation.

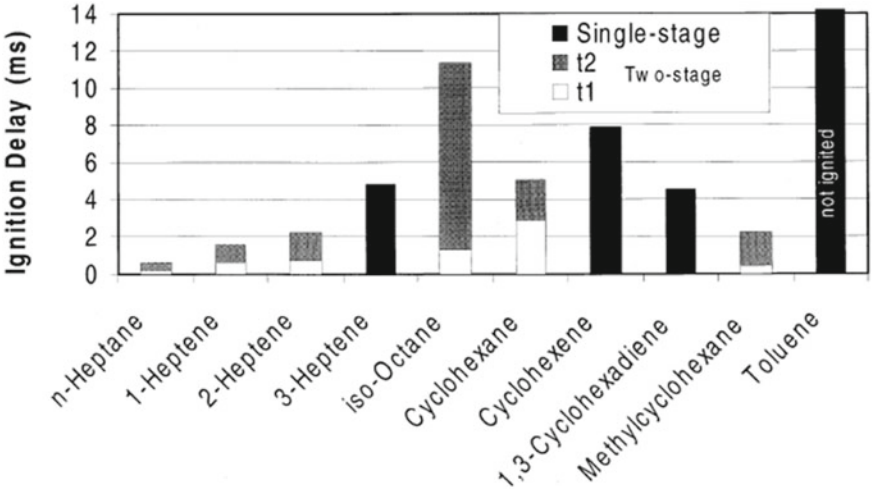

Fig. 1 Ignition delays for several fuels measured in RCM. Equivalence ratio: 0.4. Initial temperature and pressure are 318 K and 1 atm. Compression ratio: 16 From Tanaka et al. [6]

fuels (1-, 2-, and 3-heptene) compared to saturated fuel (n-heptane) and that the position of C = C bond strongly affects ignition delay. Transient ignition characteristics for these fuels in terms of pressure-time history in RCM are shown in Fig. 2. For the fuels that exhibit two-stage ignition, the 1st stage ignition is indicated by the first (smaller) peak in pressure, followed by the main or 2nd stage ignition indicated by the sharp rise in pressure. Also, the duration between the 1st stage and 2nd stage ignition becomes increasingly longer as the position of C = C bonds shifts inside for the unsaturated fuels.

Vanhove et al. [13] reported a systematic investigation on the effect of the position of the double bond on the ignition of 1-, 2-, and 3-hexene between 630 and 850 K. Figures 3 and 4 provide some results from this study, indicating generally similar ignition behavior as that observed by Tanaka et al. [6] for heptane isomers. Figure 3 plots the pressure and light emission traces after a rapid compression to 725 K and 9.4 bar for 4 different fuels. Results indicate a two-stage ignition with strong 1st stage ignition for 1-hexene, a two-stage ignition with a weak 1st stage ignition for 2-hexene, and only one-stage ignition for 3-hexene. Figure 4 shows the measured ignition delays versus gas temperature for these fuels. The data again indicates a strong effect of the position of the double bond on ignition. For 1-hexene, the behavior is generally similar to that of alkanes, i.e., two-stage ignition up to 800 K and a small NTC region between 750–830 K. For 2-hexene, these features become less clear showing a two-stage ignition with a weak 1st stage ignition that disappears above 730 K, and no NTC behavior but rather ignition delay decreasing slowly between 720 and 815 K. For 3-hexene, there is no two-stage ignition or NTC behavior, but only a faint inflection point near 730 K. Thus, the fuel ignitability is strongly influenced by the length of the saturated portion aside the double bond, with the longer alkyl

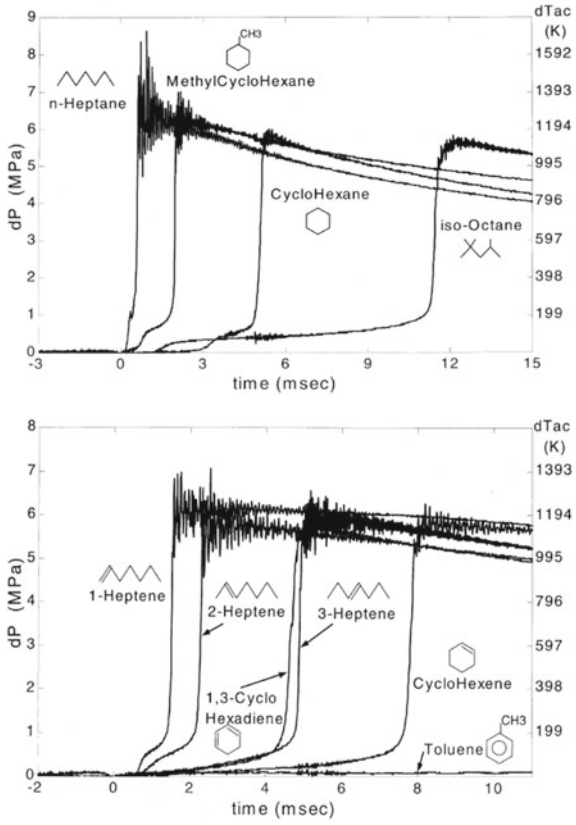

Fig. 2 RCM ignition and combustion characteristics of some saturated and unsaturated hydrocarbons. Initial temperature and pressure are 318 K and 1 atm. Compression ratio: 16 From Tanaka et al. [6]

chain yielding shorter ignition delay. Vanhove et al. [13] attributed this behavior of long-chain alkenes to a competition between the reactivity of double bond and that of alkenyl chain. For short alkenyl chains, such as in 3-hexene, the ignition is dominated by the reactivity of the double bond, while for long chains, such as in 1-hexene, it is dominated by the reactivity of alkenyl chain, resulting in two-stage ignition.

Mehl et al. [17] developed a detailed kinetic model for the oxidation of 1-, 2-, and 3-hexene and analyzed reaction pathways associated with their ignition chemistry in the temperature range of 660–1770 K. Consistent with experimental data, the reactivity of isomers was found to be strongly influenced by the position of the double bond, especially at low temperatures. Figure 5 compares their simulated ignition delays with the RCM data of Vanhove et al. [13], indicating a similar effect of the position of double bond on ignition as discussed above. Garner et al. [18] reported shock tube experiments and modeling study for the ignition of n-heptane, 1-heptene, 1, 6-heptadiene, and two C8 methyl esters, namely methyl octanoate and methyl trans-2-octenoate. Note that n-heptane and 1-heptane represent the hydrocarbon side chains of the C8 saturated and unsaturated methyl esters, respectively. Consistent with

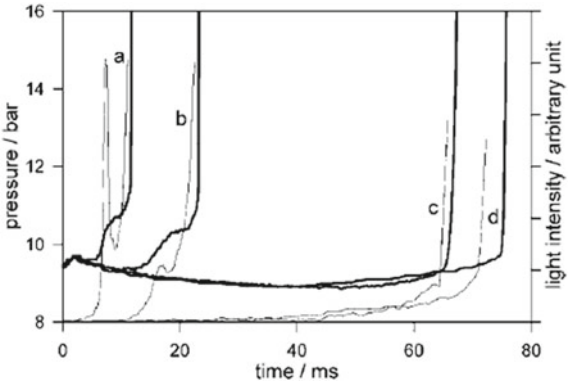

Fig. 3 Pressure (thick line) and light emission (thin line and arbitrary unit) traces after a rapid compression to 725 K and 9.4 bar for 1-hexene (**a**), 2-hexene (**b**), cyclohexene (**c**), and 3-hexene (**d**) From Vanhove et al. [13]

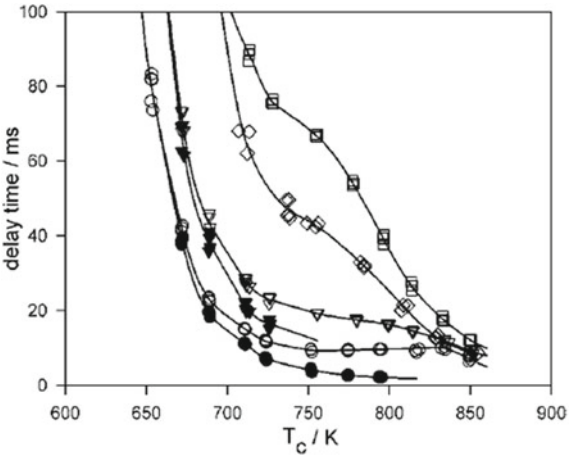

Fig. 4 1st stage (black symbols) and total (white symbols) delay times versus gas temperature for 1-hexene (circle), 2-hexene (triangle), cyclohexene (diamond), and 3-hexene (square) From Vanhove et al. [13]

previous studies, results indicated longer ignition delays as the degree of unsaturation was increased.

Westbrook et al. [19] employed a detailed kinetic mechanism to characterize the effect of C=C bond on the ignition behavior of five methyl ester compounds, namely methyl palmitate, methyl stearate, methyl oleate, methyl linoleate, and methyl linolenate, which are important components of many biodiesel fuels derived from different vegetable oils and animal fats. Methyl palmitate ($C_{17}H_{34}O_2$) and methyl stearate ($C_{19}H_{38}O_2$) contain a saturated straight chain of 15 and 17 C atoms respectively, whereas the other three components have straight chains of 17 C atoms with one C=C double bond in methyl oleate ($C_{19}H_{36}O_2$), two double bonds in methyl linoleate ($C_{19}H_{34}O_2$), and three double bonds in methyl linolenate ($C_{19}H_{32}O_2$).

Figure 6 compares the computed ignition delays for these components using stoichiometric fuel/air mixtures at 13.5 bar initial pressure. Ignition data is also included (shown as square and circle symbols for soy methyl ester (SME) and rapeseed methyl ester (RME) mixtures). Also for reference, the computed results are shown for

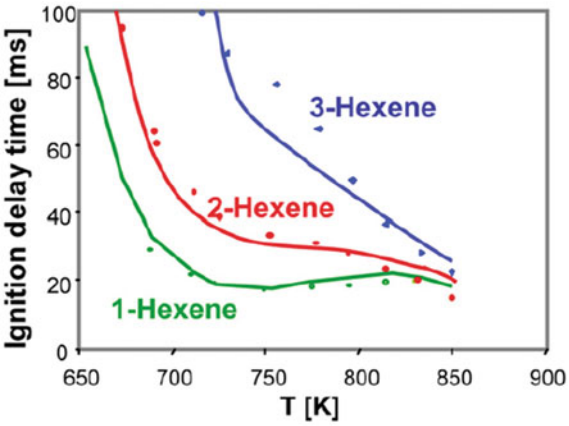

Fig. 5 RCM ignition delay times of hexene isomers (p = 0.86–1.09 MPa, Φ = 1): experiments (symbols) and calculations (lines) From Mehl et al. [17]

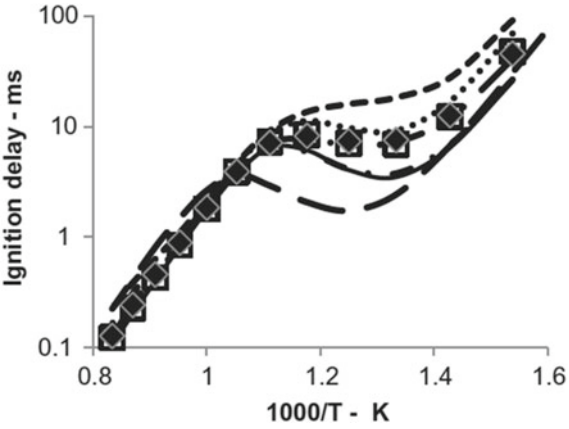

Fig. 6 Computed ignition delay times for biodiesel components, stearate (solid line), palmitate (dot-dash), oleate (dashes), linoleate (dotted), and linolenate (short dashes). Symbols show computed results for SME (squares) and RME (diamonds). Results for n-cetane are shown as long dashes. Mixtures are stoichiometric, at constant volume, and at 13.5 bar From Westbrook et al. [19]

n-cetane, which has much shorter ignite delay than any of the biodiesel components or composite fuels. Results for the five biodiesel components clearly indicate that their ignitability is adversely affected as the number of C = C bonds increases. Moreover, the effect is most pronounced in the NTC region. Thus, methyl linolenate with 3 C = C bonds is slowest to ignite, followed by methyl linoleate and methyl oleate. The ignition delays of both SME and RME are nearly the same as those of methyl oleate and methyl linoleate, which are the major components of these biodiesel fuels. As expected, both saturated components, methyl stearate and palmitate, are the fastest components to ignite, with ignition delays that are effectively identical.

Thus, ignition data for saturated and unsaturated components of petroleum-based and biodiesel fuels indicate that the number and position of the double bond has a strong effect on the reaction pathways responsible for the 1st stage ignition, total ignition delay, and the dependence of the ignition delay time on mixture temperature. In general, the presence of C = C double bond inhibits low-temperature reactivity,

increases ignition delay times, and leads to reductions in CN number in diesel engines, compared with corresponding saturated fuel molecules.

3 Effect of Unsaturation on Ignition and Flame Structure in Sprays

Compared to homogeneous, premixed systems, the fuel unsaturation and chemistry effects on ignition are much less investigated and understood for nonpremixed systems, especially those involving droplets and sprays. For droplets, additional complexities are due to the coupled two-phase processes, gas-phase convection, droplet heating and vaporization. Much of the experimental and modeling research on droplet ignition has considered a spherically symmetric configuration [20]. As discussed in Refs. [21, 22], several of these studies have examined the temperature dependent chemistry effects, such as two-stage ignition and negative temperature coefficient (NTC) behavior. The two-stage ignition was defined through the temporal variation of temperature, with the first temperature rise marking the first-stage ignition and the second (sharper) rise indicating the second-stage ignition. However, the previous studies have not provided a clear evidence for the NTC region, and it has been surmised that the presence of non-homogeneous temperature and species field causes a transition from NTC to zero temperature coefficient (ZTC) behavior. While various researchers provide different explanations for this transition, relatively few studies provide an evidence of a ZTC region. It has been suggested that competition between the availability of fuel vapor and the reduction in mixture temperature due to evaporation plays a significant role in modifying the NTC behavior [23].

Similar to the research on droplet ignition, relatively few studies have been reported on the fuel unsaturation effects on spray ignition [24], although the general topic of spray ignition has been extensively investigated [25, 26]. This is somewhat surprising since ignition represents a critical process in CI engines, and strongly influences their combustion and emission characteristics [27, 28]. Moreover, autoignition in CI engines occurs at conditions where the two-stage ignition and NTC phenomenon are highly relevant. Fu and Aggarwal [29] investigated this phenomenon in sprays by performing 3-D, two-phase reacting flow simulations in a 1.9 L 4-cylinder engine. The CONVERGE software was used for simulating the processes of fuel injection, atomization, and spray ignition. As this engine is equipped with a 7-hole common rail injector in each cylinder, simulations considered a 1/7 (51.43°) sector of the cylinder using periodic boundary conditions at the front and back face of the sector. Additional details can be found in the cited work [29]. As the fuel is injected at a given crank angle (CA), processes of spray atomization, vaporization, and fuel–air mixing follow leading to ignition. Figure 7 from Ref. [29] depicts these processes prior to ignition by plotting the spray characteristics in the cylinder at different CA after the start of injection (SOI).

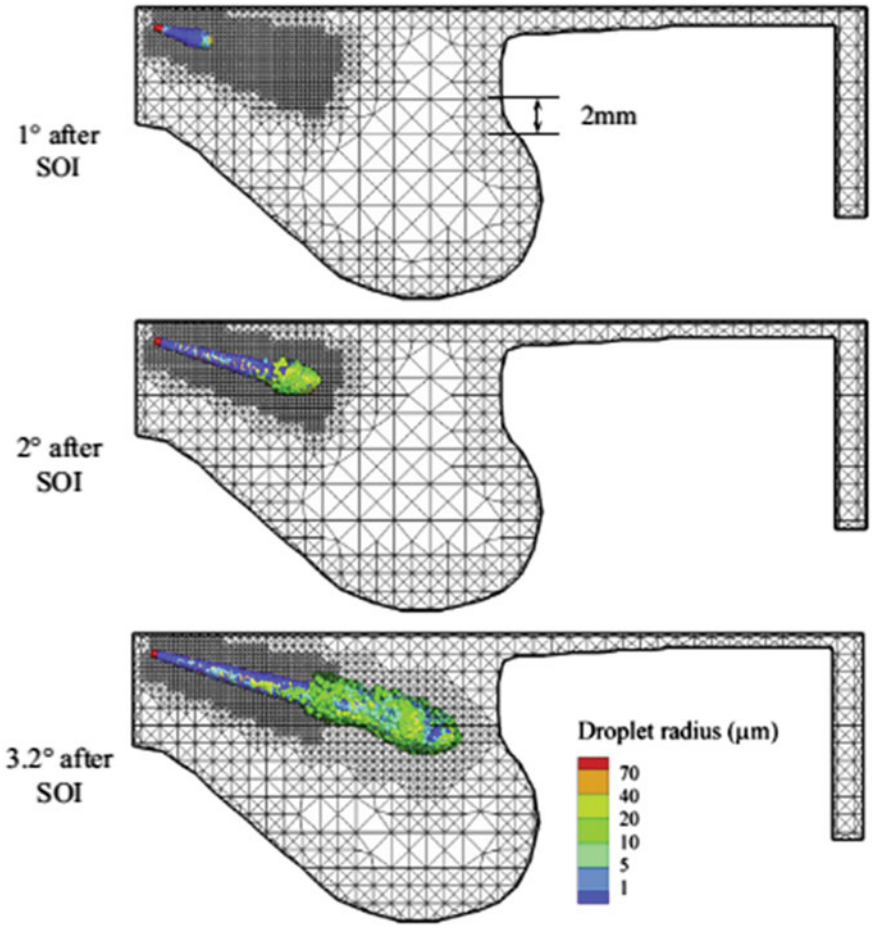

Fig. 7 A cross-section view of the cylinder through the spray, depicting the developing spray structure at 1°, 28°, and 3.28° CA after SOI, which is 8° from TDC. Each color dot represents a droplet radius in a parcel, and the size distribution is indicated by the droplet radius scale (1–70 μm) From Xu and Aggarwal [29]

The temporal and spatial behavior of the 1st and 2nd stage ignitions was analyzed through the evolution of QOOH (alkyl hydroperoxy) and OH fields, respectively, in both ϕ–T space and physical space. Note that the QOOH radicals play a key role in the chemistry of 1st stage ignition [29, 30], and its temporal evolution can be used to determine the corresponding ignition delay. Similarly, the 2nd stage ignition can be determined from the evolution of OH or HRR. A representative result from Ref. [29] is provided in Fig. 8a, which shows QOOH and OH mass profiles with respect of CA, depicting the 1st and 2nd stage ignitions for four different cases corresponding to SOI = 32°, 20°, 14°, 8° before TDC. The peak in QOOH profile determines

the 1st stage ignition, while the sharp rise (after the first peak) in OH determines the 2nd stage (main) ignition. Figure 8b plots the 1st and 2nd stage ignition delay times versus SOI for both diesel sprays and homogeneous mixtures. Note that the effect of temperature is characterized by varying SOI. As SOI is delayed, the cylinder temperature increases, and, consequently, both the 1st and 2nd stage ignition delays decrease, but the effect is stronger on the 1st stage ignition, consistent with droplet ignition results. As further discussed in Ref. [29], results indicate global similarities between the ignition processes in diesel sprays and homogeneous mixtures, but also highlight differences between them due to temporally and spatially evolving temperature and species fields for the spray case. One notable difference is that ignition in homogeneous mixtures exhibits a NTC region (see Fig. 10 in Ref. [29]), while that in diesel spray shows a near ZTC region. The transition from NTC to ZTC behavior in diesel spray is mainly due to the evolving two-phase flow, and also due to the increase in pressure during the compression stroke. In addition, the 1st and 2nd stage ignitions in sprays occur over a wide ϕ range, implying a spatially wide ignition kernel. Also, in some cases, multiple ignition kernels were observed in sprays.

In a subsequent study, Sharma and Aggarwal [31] examined the effect of fuel unsaturation on the transient ignition and flame development in n-heptane and 1-heptene turbulent sprays under diesel engine conditions. 3-D, two-phase reacting flow simulations were performed in the Sandia reactor geometry [32] by using the CONVERGE software along with a validated reaction mechanism. Results demonstrated that the spray ignition and flame structure are strongly influenced by fuel unsaturation. Details are provided in Refs. [31, 33]. Figure 9 from Ref. [33] compares the transient ignition processes in n-heptane and 1-heptene sprays in terms of the temporal variations of heat release rate (HRR), volume-integrated fuel vapor mass (m_{fv}), and QOOH and OH species mass in the reactor. Results are shown for three cases corresponding to initial temperatures of 1000, 1100, and 1200 K. As discussed in Refs. [31, 33], similar to the ignition in homogeneous mixtures, the fuel ignitability is noticeably decreased due to fuel unsaturation. As indicated in Fig. 9, the ignition delay is much longer in 1-heptene sprays than that in n-heptane sprays, especially at lower temperatures. In addition, for the 1000 and 1100 K cases, the ignition in n-heptane sprays is characterized by two-stage ignition, while in 1-heptene sprays, only the 2nd stage or main ignition is observed for all three cases. For instance, for the 1000 K n-heptane case, the 1st stage ignition occurs at 0.185 ms, followed by the main ignition at 0.325 ms. The 1st stage ignition is indicated by the first decrease in fuel vapor mass, or by the first increase in HRR in Fig. 9a, or by a sharp decrease in QOOH mass in Fig. 9c. The 2nd stage or main ignition for all the cases is indicated by a sharp decrease in fuel vapor mass, or by a sharp rise in HRR or in OH mass profile. Another notable observation is that for the range of temperatures considered, spray ignition results do not indicate any NTC region, as the ignition delay time decreases monotonically as the initial temperature is increased. Another interesting feature of spray ignition, in contrast to gaseous mixtures, is the existence of multiple ignition locations, as noted earlier. For instance, OH scatter plot at 0.3 ms in Fig. 10b indicates two ignition kernels in T-ϕ space, one near $T \approx 1100$ K and $\Phi \approx 1.6$, and the other near $T \approx 1000$ K and $\Phi \approx 2.2$.

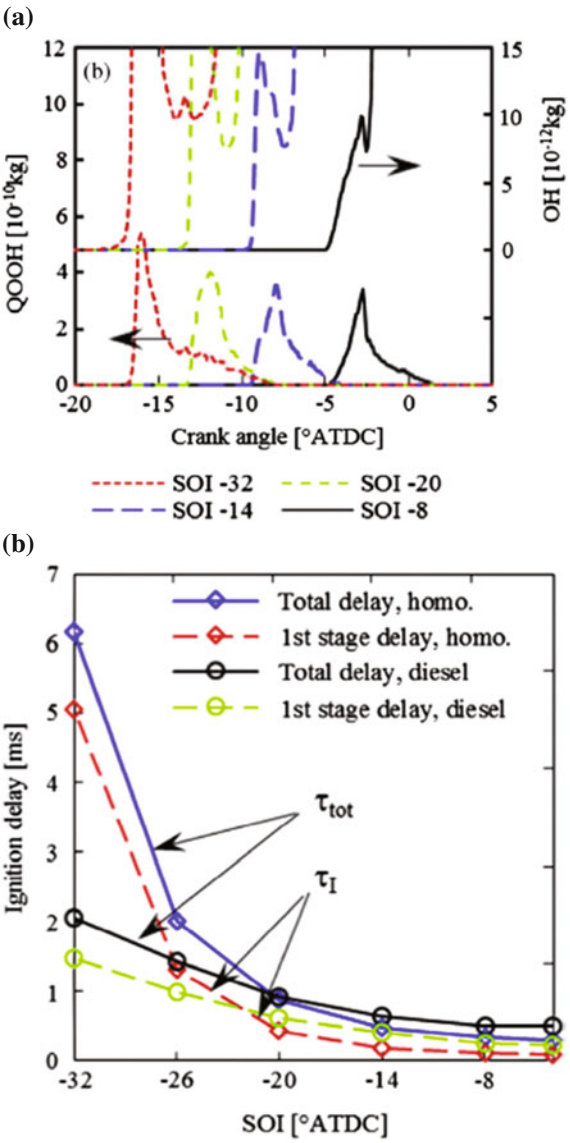

Fig. 8 **a** QOOH and OH mass profiles with respect to CA depicting the occurrence of 1st and 2nd stage ignitions for 4 cases corresponding to SOI = 32°, 20°, 14°, 8° before TDC. **b** 1st stage and 2nd stage (total) ignition delay times versus SOI for the diesel spray and homogeneous mixtures. From Xu and Aggarwal [29]

Further insight into the effect of fuel unsaturation on transient spray ignition and flame development is provided through OH scatter plots in Figs. 10 and 11 and through equivalence ratio (ϕ) and temperature (T) contours in Figs. 12 and 13. OH scatter plots in Fig. 10 again depict the two-stage ignition behavior in n-heptane spray, with the 1st and 2nd stage ignitions occurring at 0.185 ms and 0.325 ms, respectively. On the other hand, as indicated in Fig. 11, only the main ignition is observed in 1-heptene spray at 2.82 ms. Another important difference between the two fuels is

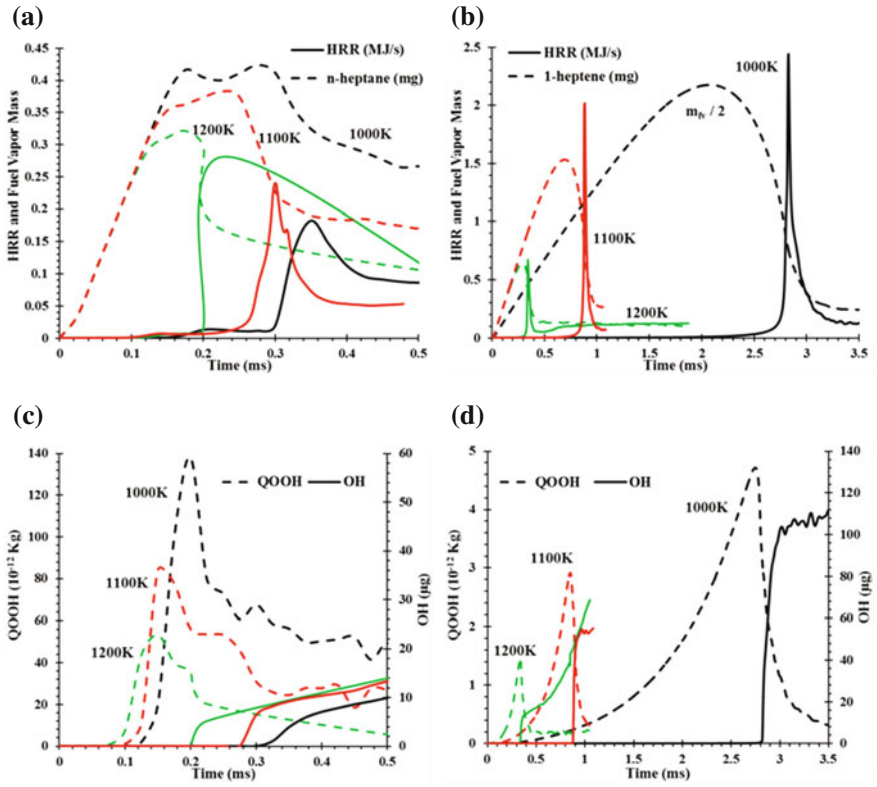

Fig. 9 Transient ignition processes in n-heptane (Fig. **a** and **c**) and 1-heptene (Fig. **b** and **d**) sprays, illustrated through the temporal variation of heat release rate (HRR), fuel vapor mass (m_{fv}), and QOOH and OH species mass for initial temperatures of 1000 K, 1100 and 1200 K. From Sharma [33]

that the main ignition in n-heptane spray occurs in rich mixtures ($1.4 < \phi < 1.6$), while that in 1-heptane involves lean mixtures ($\phi \approx 0.7$). This can be attributed to the reduced ignitability of 1-heptene, resulting in longer ignition delays and thus enhancing fuel–air mixing in case of 1-heptene. This has important consequence for the subsequent spray flame structure for the two fuels. Thus, as indicated in Figs. 12 and 13, n-heptane flame structure is characterized by two reaction zones, namely a rich premixed zone (RPZ) and a nonpremixed reaction zone (NPZ), while the 1-heptane flame is characterized by three reaction zones, i.e., a lean premixed zone (LPZ), in addition to NPZ and RPZ. These reaction zones can be visualized from the ϕ and T contour plots shown in Figs. 12 and 13 and also from HRR scatter plots in Fig. 14. For instance, the NPZ is characterized by $\phi \approx 1.0$ and high temperatures ($\approx$2350 K), whereas RPZ is characterized by ϕ between 1.3–2.1 and T between 1500–2000 K and LPZ in 1-heptene flames by ϕ between 0.6–0.9 and T between 1500–1900 K. Note that the LPZ can be identified from the OH scatter plots in

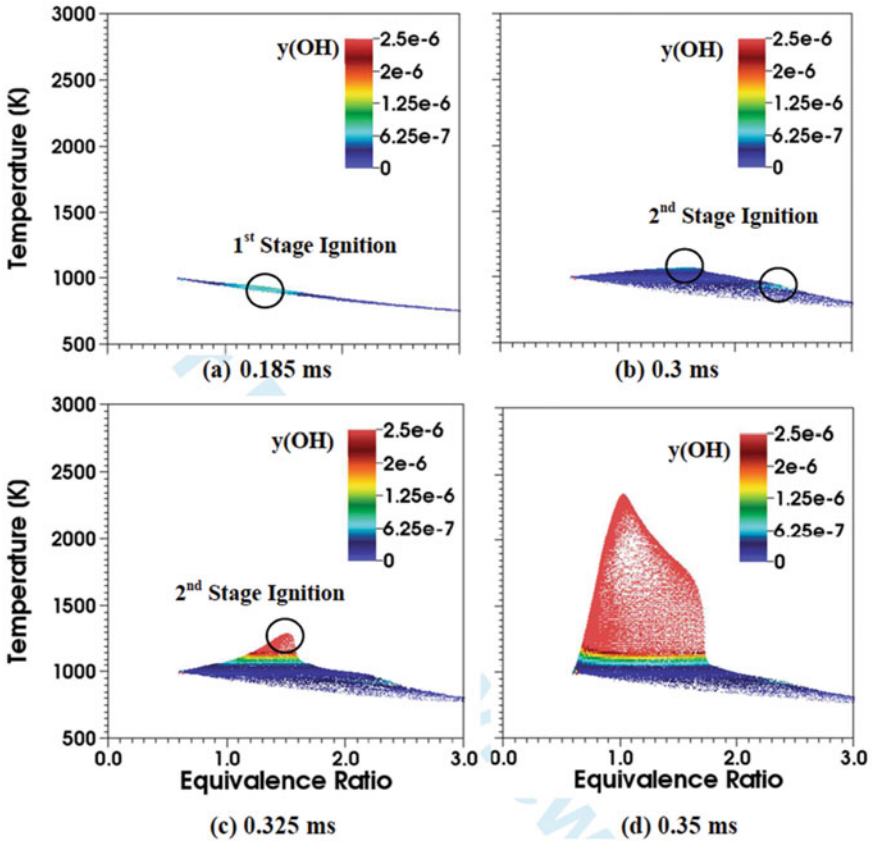

Fig. 10 Transient ignition and flame development in n-heptane spray at 1000 K; OH mass fraction scatter plots in ϕ-T space From Sharma [33]

Fig. 11, and from ϕ and T contour plots Fig. 13, and also from HRR scatter plots in Fig. 14. Thus, an important consequence of fuel unsaturation is the appearance of a lean premixed reaction zone in 1-heptene sprays, in addition to the nonpremixed and rich premixed zones.

Another important result pertains to the effect of fuel unsaturation on flame liftoff length. The flame liftoff length for various cases is indicated by a dotted vertical line in Figs. 12 and 13. The flame anchoring location downstream of the injector is determined by using a minimum OH mass fraction value of 0.02 of its peak value. For both fuels, as the ambient temperature is increased, the flame liftoff length decreases, i.e., the flame stabilization location moves closer to injector. Thus for n-heptane flames, the computed liftoff lengths are 24.5, 13, and 10.5 mm for 1000, 1100, and 1200 K, respectively. The corresponding values for 1-heptene flames are 27, 16, and 4.5 mm. It is also interesting to note that the flame liftoff position correlates with the ignition delay and ignition kernel location. Thus for 1000 and 1100 K, the liftoff

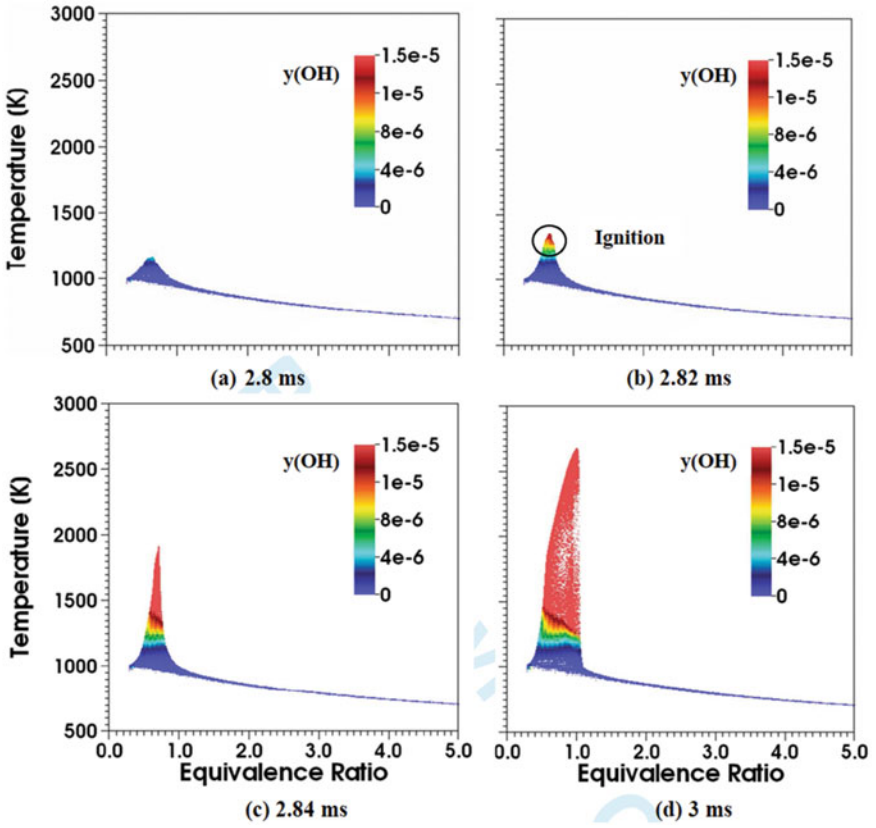

Fig. 11 Transient ignition and flame development in 1-heptene spray at 1000 K; OH mass fraction scatter plots in ϕ-T space. From Sharma [33]

lengths for 1-heptene are higher compared to those for n-heptane, since the ignition delays are longer for 1-heptene. On the other hand, for 1200 K, the liftoff length for 1-heptene is lower than that for n-heptane, since the ignition delay is shorter and the ignition kernel is located closer to injector for 1-heptene.

4 Effect of Fuel Unsaturation on NOx and Soot Emissions

This section provides a brief review of research concerning the effect of fuel unsaturation on NOx and soot emissions. Both laboratory-scale laminar flames and engine configurations are considered. Engine experiments using biodiesel fuels from different feedstock [34, 35] have observed an increase in NOx emission as the fatty acid chain length, and the number of double bonds in the fuel molecular structure

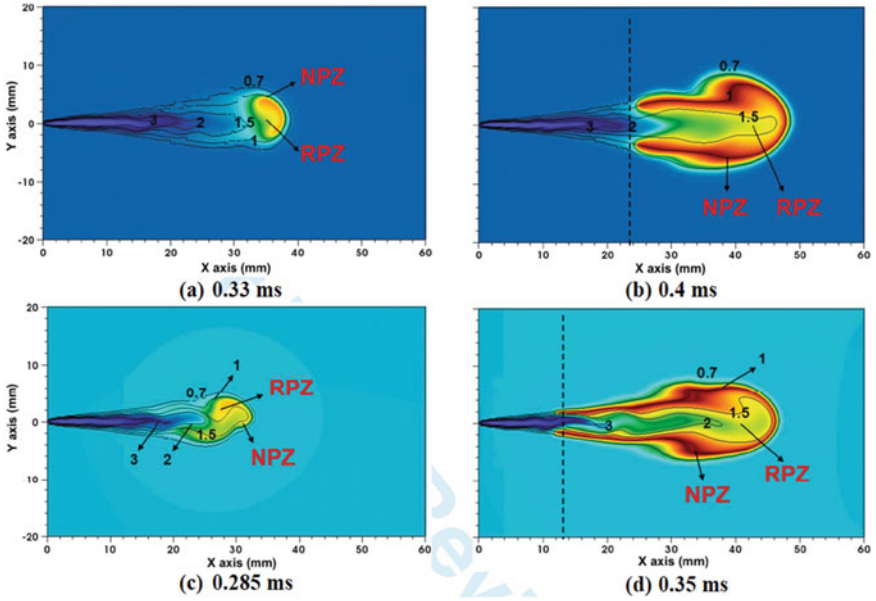

Fig. 12 Equivalence ratio (ϕ) and temperature (T) contours at different times showing the temporal evolution of n-heptane spray flames for initial temperatures of 1000 K (Fig. **a** and **b**), and 1100 K (Fig. **c** and **d**). Flooded contours indicate T between 600 to 2700 K. Contour lines represent ϕ between 0.7 and 3. Vertical line indicates the flame liftoff length. From Sharma [33].

is increased. In addition, experimental studies have reported that while PM (particulate matter) emissions are reduced using biodiesel fuels compared to conventional diesel, the amount of PM formed increases due to the presence of double bonds in the fuel molecular structure [35–37]. There have also been fundamental investigations on the emissions of NOx and soot (and their precursors) from the combustion of saturated and unsaturated biodiesel components. Garner et al. [11] reported shock tube experiments using n-heptane (n-C_7H_{16}) and 1-heptene (1-C_7H_{14}) and observed that 1-heptene produces more C_2H_2 acetylene than does n-heptane over intermediate temperatures. This has consequence for increased NOx formation through the prompt NO mechanism. Since n-heptane and 1-heptene represent the saturated and unsaturated hydrocarbon side chains of C_8 methyl esters, respectively, Garner and Brezinsky [38] and Garner et al. [18] extended the study to the oxidation of these esters and observed increased C_2H_2 formation in the case of unsaturated methyl ester. Note that C_2H_2 also provides a major route for soot particle surface growth through the "H-abstraction-C_2H_2-addition" (HACA) mechanism [39, 40].

Han et al. [41] simulated partially premixed laminar flames (PPFs) burning prevaporized n-heptane and 1-heptene fuels and observed higher amounts of acetylene and NOx in 1-heptene flames than that in n-heptane flames. As stated earlier, these fuels represent the hydrocarbon side chains of the saturated and unsaturated methyl esters, namely methyl octanoate and methyl *trans*-2-octenoate. Thus, the study was

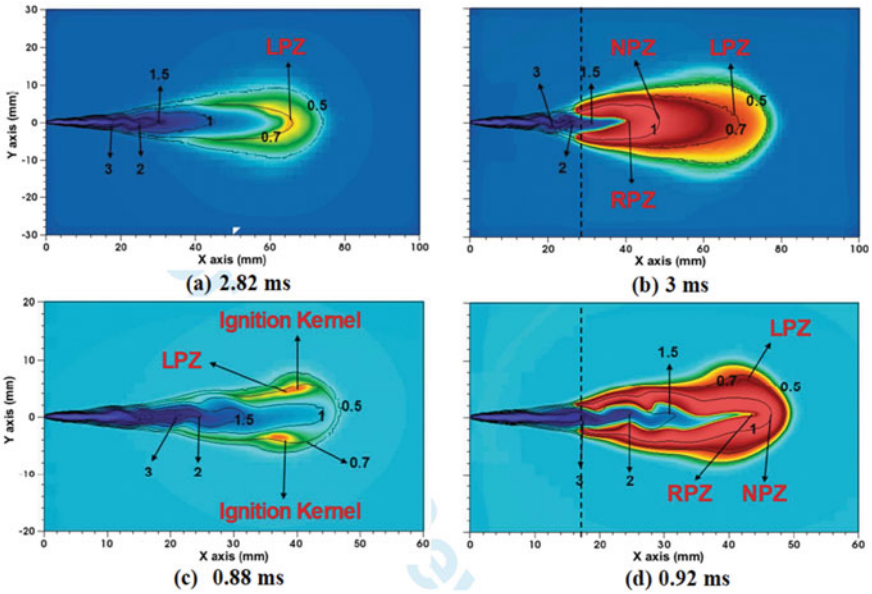

Fig. 13 Equivalence ratio (ϕ) and temperature (T) contours at different times showing the temporal evolution of 1-heptene spray flames for initial temperatures of 1000 K (Fig. **a** and **b**), and 1100 K (Fig. **c** and **d**). Flooded color contours indicate T between 600 to 2700 K. Contour lines represent ϕ between 0.7 and 3. Vertical line indicates the flame liftoff length. From Sharma [33]

also relevant to the understanding of NOx emissions from the combustion of biodiesel fuels. Triple flames were simulated in a counterflow configuration using the OPPDIF in CHEMKIN-Pro 15113 package [42]. The configuration involves two opposing, axisymmetric jets, one issuing a fuel-lean mixture and the other a fuel-rich mixture. A validated reaction mechanism [43] was used to model the n-heptane, 1-heptene oxidation chemistry. The mechanism was combined with a detailed NOx kinetics model that included sub-mechanisms for NO formation through the thermal, prompt, N_2O intermediate, NNH routes [44, 45].

A triple flame is characterized by the existence of three reaction zones, namely lean premixed zone (LPZ), rich premixed zone (RPZ), and nonpremixed reaction zone (NPZ), which are spatially separated but strongly coupled through the transport and chemical kinetic. Thus, the objective was to characterize the effect of the presence of the double bond on C_2H_2 and NOx emissions in partially premixed flames containing regions of lean premixed, rich premixed, and nonpremixed combustion. Moreover, using a counterflow geometry, the spatial separation between the three reaction zones can be controlled by varying the strain rate and the lean and rich equivalence ratios (ϕ_L and ϕ_R). Further, details are provided in Ref. [41]. One representative result from this study is shown in Fig. 15, which plots the emission indices of total NO and those formed via prompt, thermal, N_2O, and NNH routes in n-heptane and 1-heptene triple flames at different strain rates. An important observation is the higher NO emission

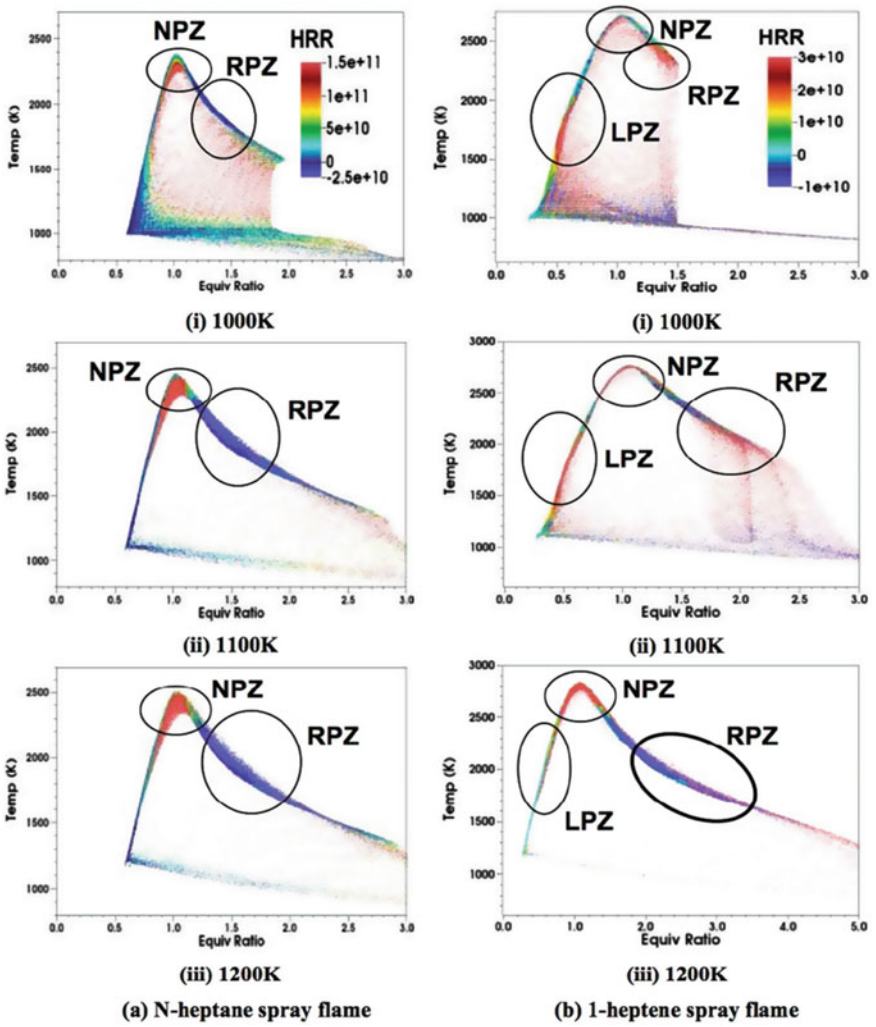

Fig. 14 HRR scatter plots in T-ϕ space for **a** n-heptane and **b** 1-heptene spray flames for initial temperatures of 1000 K (i), 1100 K (ii) and 1200 K (iii) From Sharma [33]

in 1-heptene flames compared to that in n-heptane flames irrespective of the strain rate. As discussed in Ref. [41], the reaction path analysis indicated that the β scission and oxidation reactions related to the double C = C bond lead to higher amount of C_2H_2 and thus increased NO through the prompt mechanism in 1-heptene flames compared to that in n-heptane flames. Moreover, as the strain rate is increased, the EINO first increases and then decreases, which was due to the variation of peak flame temperature with strain rate. The EI values for the prompt, thermal, N_2O, and NNH mechanisms follow a similar trend. However, the relative contribution of prompt NO

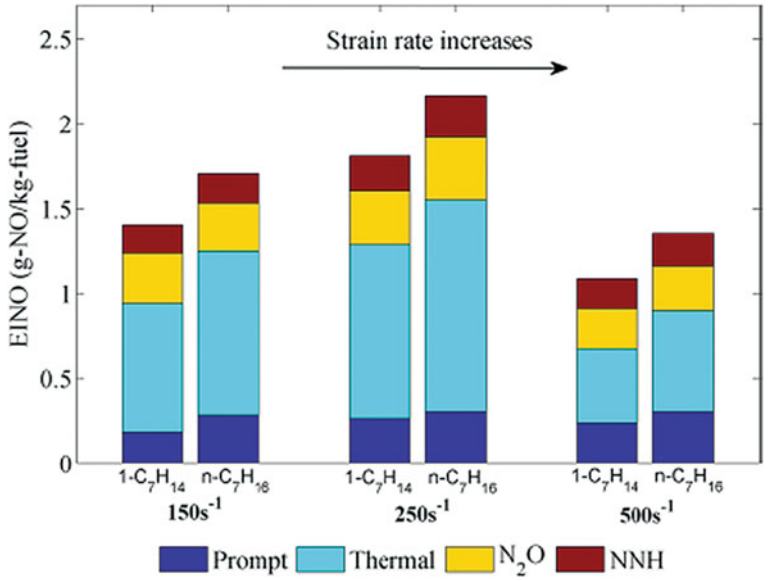

Fig. 15 Emission index for the total NO, and of NO produced through the prompt, thermal, N2O, and NNH mechanisms in n-heptane and 1-heptene triple flames established at strain rates of 150, 250, and 500 s^{-1}, and $\phi_L = 0.8$, and $\phi_R = 1.5$ From Han et al. [41]

becomes more pronounced at higher strain rates, while that of thermal NO is reduced to the lower residence time.

Fu et al. [46] extended the above investigation [41] and examined the effect of fuel unsaturation on NOx and PAH emissions in double PPFs, i.e., flames containing two reaction zones, RPZ and NPZ. The flames were again established in a counterflow geometry by issuing a fuel-rich mixture with a specified ϕ in one jet and air in the other jet. Depending upon the level of partial premixing (i.e., ϕ), a significant amount of soot formation is expected in the region between the rich premixed zone and the stagnation plane. Various PPFs were simulated by independently varying ϕ and global strain rate (a_G). One representative result from Ref. [46] is presented in Fig. 16, which shows the peak mole fractions of major soot precursor species, namely C_2H_2, benzene (C_6H_6), and pyrene ($C_{16}H_{10}$) in n-heptane and 1-heptene PPFs established at different strain rates and two levels of partial premixing with $\phi = 8$ and 2. As indicated, at any given ϕ and strain rate, the peak mole fractions of C_2H_2, C_6H_6, and $C_{16}H_{10}$ are noticeably higher in 1-heptene flames than those in n-heptane flames. Also, the effect of the double bond is more pronounced at lower ϕ (higher level of partial premixing) and higher strain rate.

Fu et al. [46] further extended this work to characterize the effect of fuel unsaturation on soot emissions in counterflow PPFs. The previously used fuel oxidation and NOx chemistry mechanism were combined with a detailed soot model [39, 40], and the combined model was validated against gaseous species measurements in n-

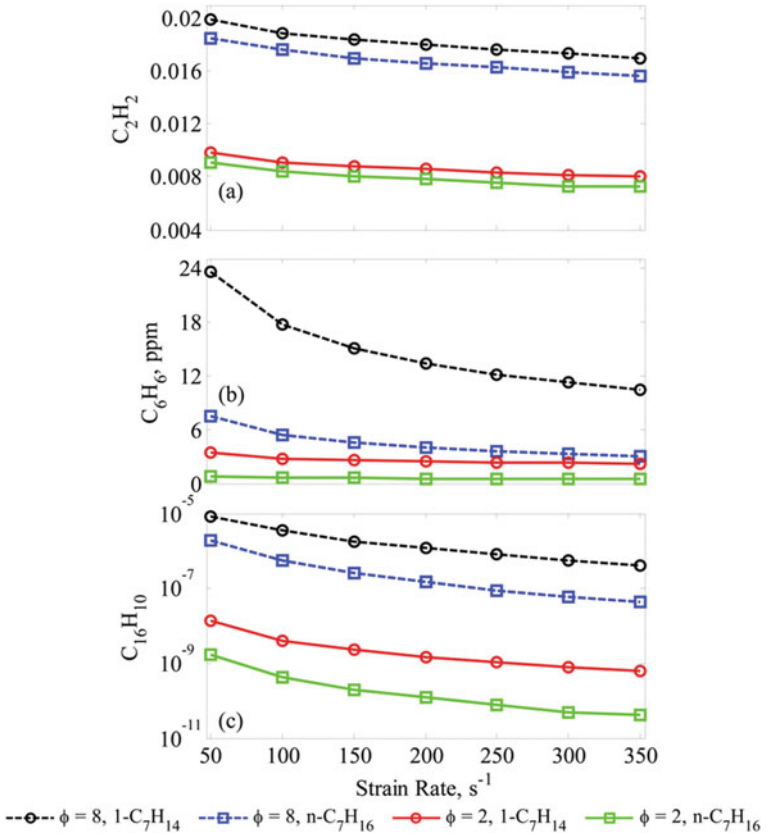

Fig. 16 Peak mole fractions of acetylene, benzene, and pyrene ($C_{16}H_{10}$) plotted versus strain rate for n-heptane and 1-heptene partially premixed flames PPFs at $\phi = 2$ and 8. Pyrene is plotted on a log scale From Fu et al. [46]

heptane PPFs and soot measurements in ethylene diffusion flames. Simulations were then performed to examine the effects of double bonds on PAHs and soot emissions at different strain rates and levels of premixing. A representative result from Ref. [46] is shown in Fig. 17, which plots the soot properties in n-heptane and 1-heptene PPFs established at different strain rates and two levels of partial premixing with $\phi = 8$ and 2. These results should be viewed along with those presented in Fig. 16, which indicated that at any given ϕ and strain rate, the amounts of soot precursor species (C_2H_2, C_6H_6, and $C_{16}H_{10}$) formed in 1-heptene flames are markedly higher than those in n-heptane flames. Consequently, as indicated in Fig. 17, the soot particle diameter, soot volume fraction, and number density are significantly higher in 1-heptene flames than those in n-heptane flames. Also, similar to soot precursor species, the effect of the double bond on soot becomes more significant as the strain rate and/or the level of premixing are increased (i.e., ϕ in the fuel jet is reduced).

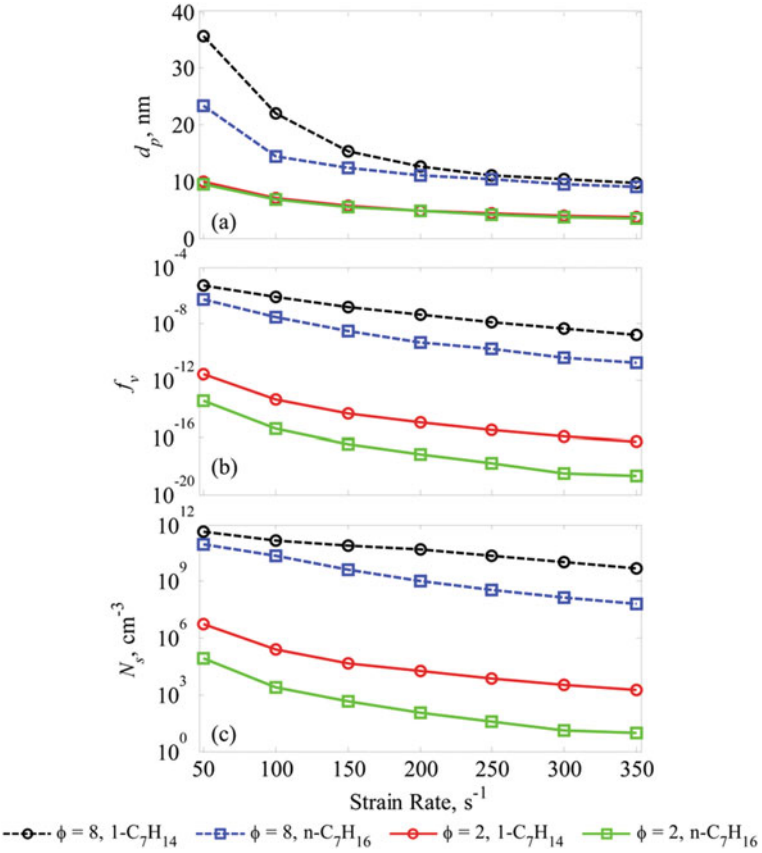

Fig. 17 Peak soot diameter (**a**), number density (**b**), and volume fraction (**c**) plotted versus strain rate for n-heptane and 1-heptene partially premixed flames at $\phi = 2$ and 8. Number density and volume fraction are on a log scale, and soot diameter is on a linear scale. From Fu et al. [46]

Further, analysis indicated that the increased soot emission is related to the higher nucleation and surface growth rates, which are due to the increased production of $C_{16}H_{10}$ and C_2H_2 in 1-heptene flames compared to that in n-heptane flames. The increased production of $C_{16}H_{10}$ is due to the higher amount of C_6H_6 in 1-heptene flames.

A reaction path analysis was performed to identify the dominant routes for the formation of acetylene, benzene, and pyrene. Acetylene and benzene are known to be important precursors for larger PAH species, while acetylene also plays an important role in soot surface growth through the HACA mechanism. The analysis indicated that the major route for benzene formation in the RPZ is through the recombination reaction of propargyl radicals, which are mostly formed from allyl radicals. The other route is through the reaction of vinyl with butadiene. The presence of double bond leads to higher concentrations of propargyl and butadiene and thus increased

benzene formation in 1-heptene flames than in n-heptane flames. The presence of double bond also increases the amount of C_2H_2 formed in 1-heptene flames due to the higher C_4H_5 concentration. Thus, the presence of double bond promotes scission β reactions leading to the increased production of C_2H_2, C_6H_6, and $C_{16}H_{10}$ and thus higher soot emissions in 1-heptene flames.

As mentioned earlier, there is relatively little work reported dealing with unsaturation effects in spray flames, except for engine experiments with biodiesel fuels. Fu and Aggarwal [48] recently reported a computational study on the effect of fuel unsaturation on NOx and PAH emission in turbulent spray flames under diesel engine conditions. N-heptane and 1-heptane spray flames in the Sandia reactor [32] were computed using the CONVERGE software. A reduced mechanism was developed starting from the detailed CRECK mechanism using the directed relation graph methodology. The mechanism was validated using the shock tube ignition data and reacting spray data from the Engine Combustion Network [32]. Further, details of the two-phase models and operating conditions are provided in Ref. [48]. Results indicated that the combustion in Sandia reactor is characterized by a double-flame structure with a rich premixed reaction zone (RPZ) near the flame stabilization region and a nonpremixed reaction zone (NPZ) further downstream. Most of NOx is formed in NPZ, while PAH species are mainly formed in RPZ. The presence of double bond leads to higher flame temperature and thus higher NO in 1-heptene flame than that in n-heptane flame. It also leads to the increased formation of PAH species, implying increased soot emission in 1-heptene flame than that in n-heptane flame. A representative result from Ref. [48] is shown in Fig. 18, which compares the temporal variation of volume-integrated NO, benzene and pyrene mass in n-heptane and 1-heptene flames. As indicated, 1-heptene flame produces significantly more NO and PAH species compared to n-heptane flame. For instance, at $t = 1.4$ ms, there is 20% more NO, 22.0% more benzene, and 21.9% more pyrene in 1-heptane flames. Figure 19 shows the spatial distribution of benzene in terms of its mass fraction contours for the two flames at $t = 1.4$ ms. The benzene formation region is located within the rich premixed zone for both flames, and the amount of benzene formed in 1-heptene is significantly higher. The peak mass fractions are 0.0118 and 0.0087 for 1-heptene and n-heptane, respectively, i.e., 36% higher benzene for 1-heptene. Similar trends were observed for the formation of heavier PAH, such as pyrene. Reaction path analysis indicates that the increased formation of PAH species can be attributed to the significantly higher amounts of 1,3-butadiene and allene formed due to β scission reactions resulting from the presence of double bond in 1-heptene.

5 Conclusions

A review of research dealing with the effects of fuel unsaturation on the ignition, combustion, and emission characteristics has been provided. Results from both laboratory-scale configurations, such as shock tube (ST), rapid compression machine (RCM), and laminar flames, as well as from high-pressure sprays in compression

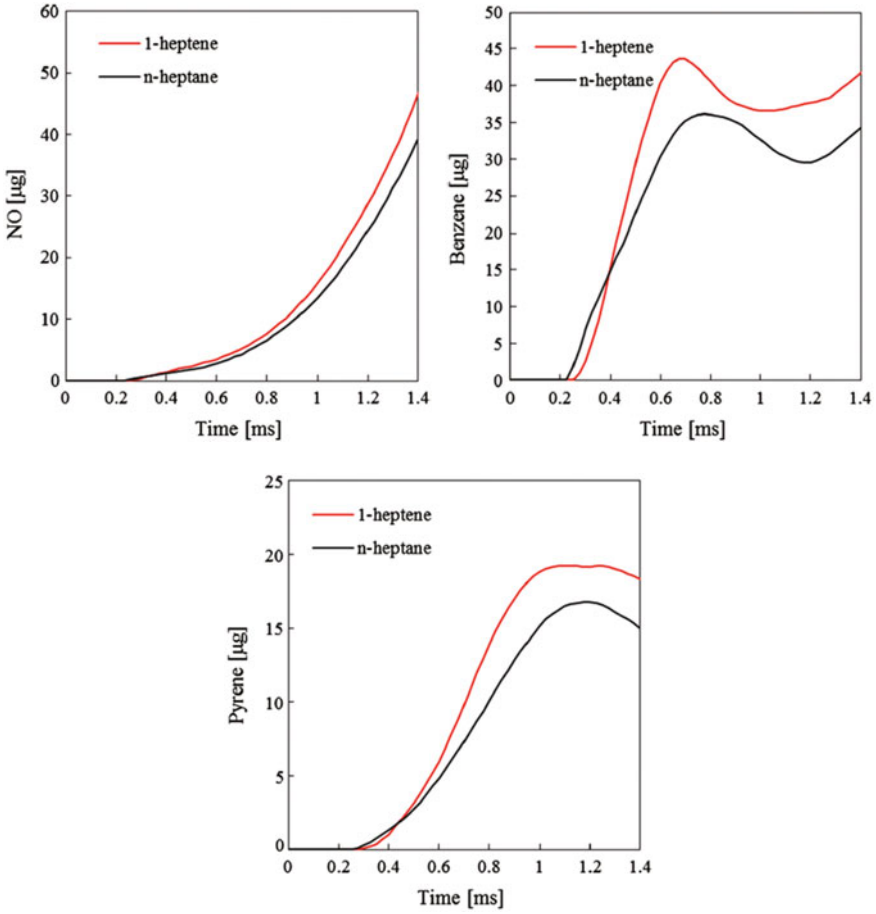

Fig. 18 Volume-integrated NO, benzene, and pyrene mass plotted versus time for n-heptane (black) and 1-heptane (red) spray flames in the Sandia reactor. Initial temperature is 1300 K From Fu and Aggarwal [48]

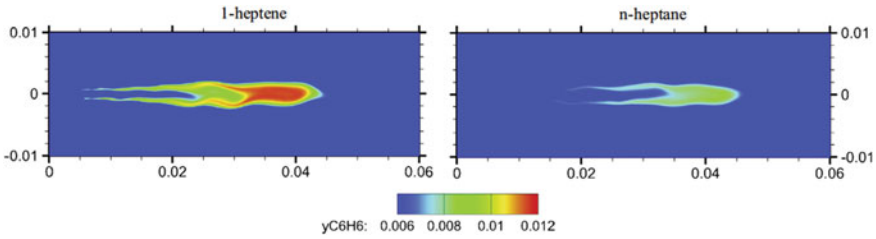

Fig. 19 Benzene mass fraction contours for 1-heptene and n-heptane flames at 1.4 ms. Mass fractions are between 0.006 and 0.012. Dimensions are in m Fu and Aggarwal [48]

ignition engines are discussed. Experimental and kinetic modeling studies provide clear evidence that depending upon the number and position of C = C double bonds, and the reactivity of long-chain hydrocarbons is significantly affected by fuel unsaturation, especially at low to intermediate temperatures that include the NTC region. Ignition data for homogeneous mixtures indicate that the presence of double bond has a strong effect on the 1st stage ignition, reduces low-temperature reactivity significantly, increases total ignition delay time, and leads to reduction in CN number in diesel engines. This has important consequences regarding the effect of unsaturation on the combustion and emission behavior in engines.

Results for n-heptane and 1-heptene diesel sprays indicate that at low to intermediate temperatures, ignition delays are longer for 1-heptene compared to those for n-heptane. Also, ignition in n-heptane sprays occurs in fuel-rich mixtures and is characterized by a two-stage ignition process. On the other hand, ignition in 1-heptene sprays occurs in lean mixtures, without any evidence of two-stage ignition. Consequently, the n-heptane flame contains two reaction zones, i.e., a rich premixed zone (RPZ) and a nonpremixed reaction zone (NPZ), while the 1-heptene flame contains three reaction zones, i.e., a lean premixed zone (LPZ) in addition to NPZ and RPZ. Also at lower temperatures, the flame liftoff length in 1-heptene spray is greater than that in n-heptane spray, while at higher temperatures, the liftoff length is smaller in 1-heptene spray.

Results for counterflow, partially premixed flames (PPF) indicate higher amounts of NOx and soot precursor species (C_2H_2, C_6H_6, and $C_{16}H_{10}$) formed in 1-heptene flames than those in n-heptane flames. Consequently, the soot emission (i.e., soot particle diameter, volume fraction, and number density) in 1-heptene flames is higher than that in n-heptane flames. Moreover, the effect of double bond on soot emission becomes more pronounced as the strain rate or the level of premixing is increased. Simulations of turbulent n-heptane and 1-heptene spray flames in diesel engines lead to similar conclusions regarding the effect of fuel unsaturation on emission, i.e., higher NOx and soot emissions in 1-heptene flames. Reaction path analysis indicates that the increased formation of PAH species can be attributed to the significantly higher amounts of 1,3-butadiene and allene formed due to β scission reactions resulting from the presence of double bond in 1-heptene.

Acknowledgements Most of the results presented in this chapter are from the work of my graduate students as part of their thesis research. In particular, I acknowledge the contributions of Dr. Sibendu Som, Dr. Xiao Fu, Mr. Xu Han, and Mr. Saurabh Sharma. The help provided by Dr. P. K. Senecal and his colleagues at Convergent Science in using the Converge code is also greatly appreciated. Many of the simulations were performed at the UIC High Performance Computing Cluster.

References

1. C.K. Westbrook, W.J. Pitz, S.M. Sarathy, M. Mehl, Detailed chemical kinetic modeling of the effects of CC double bonds on the ignition of biodiesel fuels. Proc. Combust. Inst. **34**, 3049–3056 (2013)
2. M.S. Graboski, R.L. McCormick, Combustion of fat and vegetable oil derived fuels in diesel engines. Prog. Energy Combust. Sci. **24**, 125–164 (1998)
3. G. Kalghatgi, H. Babiker, J. Badra, A simple method to predict knock using toluene, n-heptane and iso-octane blends (TPRF) as gasoline surrogates. SAE Int. J. Eng. **8**, 505–519 (2015)
4. T. Javed, C. Lee, M. Al Abbad, K. Djebbi, M. Beshir, J. Badra, H. Curran, A. Farooq, Ignition studies of n-heptane/iso-octane/toluene blends. Combust. Flame **171**, 223–233 (2016)
5. T. Javed, E.F. Nasir, A. Ahmed, J. Badra, K. Djebbi, M. Beshir, W. Ji, S.M. Sarathy, A. Farooq, Ignition delay measurements of light naphtha: a fully blended low octane fuel. Proc. Combust. Inst. **36**(1), 315–322 (2017)
6. S. Tanaka, F. Ayala, J.C. Keck, J.B. Heywood, Two-stage ignition in HCCI combustion and HCCI control by fuels and additives. Combust. Flame **132**, 219–239 (2003)
7. CHEMKIN-PRO 15141, Reaction Design, San Diego, 2015
8. D.G. Moffat, K. Harry, R.L. Speth, Cantera: an object- oriented software toolkit for chemical kinetics, thermodynamics, and transport processes (2017), http://www.cantera.org. Version 2.3.0. https://doi.org/10.5281/zenodo.170284
9. S. Touchard, F. Buda, G. Dayma, P.A. Glaude, R. Fournet, F. Battin-Leclerc, Int. J. Chem. Kinet. **37**(8), 451–463 (2005)
10. M. Mehl, W.J. Pitz, C.K. Westbrook, K. Yasunaga, C. Conroy, H.J. Curran, Autoignition behavior of unsaturated hydrocarbons in the low and high temperature regions. Proc. Combust. Inst. **33**, 201–208 (2011)
11. S. Garner, R. Sivaramakrishnan, K. Brezinsky, The high-pressure pyrolysis of saturated and unsaturated C7 hydrocarbons. Proc. Combust. Inst. **32**, 461–467 (2009)
12. R. Minetti, A. Roubaud, E. Therssen, M. Ribaucour, L.R. Sochet, The chemistry of pre-ignition of n-pentane and 1-pentene. Combust. Flame **118**, 213–220 (1999)
13. G. Vanhove, M. Ribaucour, R. Minetti, On the influence of the position of the double bond on the low-temperature chemistry of hexenes. Proc. Combust. Inst. **30**, 1065–1072 (2005)
14. S.K. Prabhu, R.K. Bhat, D.L. Miller, N.P. Cernansky, 1-Pentene oxidation and its interaction with nitric oxide in the low and negative temperature coefficient regions. Combust. Flame **104**, 377–391 (1996)
15. M. Pelucchi, M. Bissoli, C. Cavallotti, A. Cuoci, T. Faravelli, A. Frassoldati, E. Ranzi, A. Stagni, Improved kinetic model of the low-temperature oxidation of n-heptane. Energy Fuels **28**(11), 7178–7193 (2014)
16. E. Ranzi, A. Frassoldati, R. Grana, A. Cuoci, T. Faravelli, A.P. Kelley, C.K. Law, Hierarchical and comparative kinetic modeling of laminar flame speeds of hydrocarbon and oxygenated fuels. Prog. Energy Combust. Sci. **38**(4), 468–501 (2012)
17. M. Mehl, G. Vanhove, W.J. Pitz, E. Ranzi, Oxidation and combustion of the n-hexene isomers: a wide range kinetic modeling study. Combust. Flame **155**, 756–772 (2008)
18. S. Garner, T. Dubois, C. Togbe, N. Chaumeix, P. Dagaut, K. Brezinsky, Biologically derived diesel fuel and NO formation: Part 2: model development and extended validation. Combust. Flame **158**, 2302–2313 (2011)
19. C.K. Westbrook, W.J. Pitz, S.M. Sarathy, M. Mehl, Detailed chemical kinetic modeling of the effects of C = C double bonds on the ignition of biodiesel fuels. Proc. Combust. Inst. **34**(2), 3049–3056 (2013)
20. S.K. Aggarwal, Single droplet ignition: theoretical analyses and experimental findings. Prog. Energ Combust. Sci. (2014). https://doi.org/10.1016/j.pecs.2014.05.002
21. O. Moriue, C. Eigenbrod, H.J. Rath, J. Sato, K. Okai, M. Tsue, M. Kono, Effects of dilution by aromatic hydrocarbons on staged ignition behavior of n-decane droplets. Proc. Combust. Inst. **28**, 969–975 (2000)

22. A. Cuoci, M. Mehl, G. Buzzi-Ferraris, T. Faravelli, D. Manca, E. Ranzi, Autoignition and burning rates of fuel droplets under microgravity. Combust. Flame **143**, 211–226 (2005)
23. Z. Bouali, C. Pera, J. Reveillon, Numerical analysis of the influence of two-phase flow mass and heat transfer on n-heptane autoignition. Combust. Flame **159**, 2056–2068 (2012)
24. M.C. Wolff, J. Meisl, R. Koch, S. Wittig, The influence of evaporation on the autoignition-delay of n-heptane air mixtures under gas turbine conditions. Proc. Combust. Inst. **27**, 2025–2031 (1998)
25. S.K. Aggarwal, A review of spray ignition phenomenon: present status and future research. Prog. Energy Combust. Sci. **24**, 565–600 (1998)
26. E. Mastorakos, Ignition of turbulent non-premixed flames. Prog. Energy Combust. Sci. **35**, 57–97 (2009)
27. L.M. Pickett, S. Kook, H. Persson, O. Andersson, Diesel fuel jet lift-off stabilization in the presence of laser-induced plasma ignition. Proc. Combust. Inst. **32**, 2793–2800 (2009)
28. S. Som, S.K. Aggarwal, Effects of primary breakup modeling on spray and combustion characteristics of compression ignition engines. Combust. Flame **157**, 1179–1193 (2010)
29. X. Fu, S.K. Aggarwal, Two-stage ignition and NTC phenomenon in diesel engines. Fuel **144**, 188–196 (2015)
30. H.J. Curran, W.J. Pitz, C.K. Westbrook, C.V. Callahan, F.L. Dryer, Oxidation of automotive primary reference fuels at elevated pressures. Proc. Combust. Inst. **27**, 379–387 (1998)
31. S. Sharma, S.K. Aggarwal, Effects of fuel unsaturation on transient ignition and flame development in sprays. Combust. Sci. Technol. (2017). https://doi.org/10.1080/00102202.2017.1378649
32. Engine Combustion Network (ECN), diesel sprays data search utility (2015), http://www.sandia.gov/ecn/cvdata/dsearch/frameset.php. Accessed Feb 2015
33. S. Sharma, A numerical study of transient ignition and flame structure in diesel sprays in a constant volume reactor, M.S. thesis, Department of Mechanical and Industrial Engineering, University of Illinois at Chicago, Chicago, Illinois, 2017
34. R.L. McCormick, M.S. Graboski, T.L. Alleman, A.M. Herring, K.S. Tyson, Impact of biodiesel source material and chemical structure on emissions of criteria pollutants from a heavy-duty engine. Environ. Sci. Technol. **35**(9), 1742–1747 (2001)
35. S. Puhan, N. Saravanan, G. Nagarajan, N. Vedaraman, Effect of biodiesel unsaturated fatty acid on combustion characteristics of a DI compression ignition engine. Biomass Bioenerg. **34**, 1079–1088 (2010)
36. M. Lapuerta, J.M. Herreros, L.L. Lyons, R. García-Contreras, Y. Briceño, Effect of the alcohol type used in the production of waste cooking oil biodiesel on diesel performance and emissions. Fuel **87**, 3161–3169 (2008)
37. A. Schönborn, N. Ladommatos, J. Williams, R. Allan, J. Rogerson, The influence of molecular structure of fatty acid monoalkyl esters on diesel combustion. Combust. Flame **156**, 1396–1412 (2009)
38. S. Garner, K. Brezinsky, Biologically derived diesel fuel and NO formation: an experimental and chemical kinetic study, Part 1. Combust. Flame **158**, 2289–2301 (2011)
39. M. Frenklach, H. Wang, Proc. Combust. Inst. **23**, 1559 (1991)
40. M. Frenklach, Reaction mechanism of soot formation in flames. Phys. Chem. Chem. Phys. **4**, 2028–2037 (2002)
41. X. Han, S.K. Aggarwal, K. Brezinsky, Effect of unsaturated bond on NOx and PAH formation in n-Heptane and 1-Heptene triple flames. Energy Fuels **27**, 537–548 (2013)
42. A.E. Lutz, R.J. Kee, J.F. Grcar, FM. Rupley, OPPDIF: a FORTRAN program for computing opposed flow diffusion flames. Sandia Natl. Lab. [Tech. Rep.] SAND 96−8243, UC-1404 (1997)
43. E. Ranzi, M. Dente, A. Goldaniga, G. Bozzano, T. Faravelli, Lumping procedures in detailed kinetic modeling of gasification, pyrolysis, partial oxidation and combustion of hydrocarbon mixtures. Prog. Energy Combust. Sci. **27**, 99–139 (2001)
44. J.A. Miller, C.T. Bowman, Mechanism and modeling of nitrogen chemistry in combustion. Prog. Energy Combust. Sci. **15**, 287–338 (1989)

45. J.W. Bozzelli, A.M. Dean, O+NNH: a possible new route for NOx formation in flames. Int. J. Chem. Kinet. **27**, 1097–1109 (1995)
46. X. Fu, S. Garner, S.K. Aggarwal, K. Brezinsky, Numerical study of NO_x emissions from n-heptane and 1-heptene counterflow flames. Energy Fuels **26**, 879–888 (2012)
47. X. Fu, X. Han, K. Brezinsky, S.K. Aggarwal, Effect of fuel molecular structure and premixing on soot emissions from n-heptane and 1-heptene flames. Energy Fuels **27**(10), 6262–6272 (2013)
48. X. Fu, S.K. Aggarwal, Fuel unsaturation effects on NOx and PAH formation in spray flames. Fuel **160**, 1–15 (2015)